

Long-range coupling and scalable architecture for superconducting flux qubits

Austin G. Fowler¹, William F. Thompson¹, Zhizhong Yan¹, Ashley M. Stephens² and Frank K. Wilhelm¹

¹*Institute for Quantum Computing,*

University of Waterloo, Waterloo, ON, CANADA

²*Centre for Quantum Computer Technology,*

University of Melbourne, Victoria, AUSTRALIA

(Dated: May 27, 2019)

Constructing a fault-tolerant quantum computer is a daunting task. Given any design, it is possible to determine the maximum error rate of each type of component that can be tolerated while still permitting arbitrarily large-scale quantum computation. It is an underappreciated fact that including an appropriately designed mechanism enabling long-range qubit coupling or transport substantially increases the maximum tolerable error rates of all components. With this thought in mind, we take the superconducting flux qubit coupling mechanism described in [1] and extend it to allow approximately 500 MHz coupling of square flux qubits, 50 μm a side, at a distance of up to several mm. This mechanism is then used as the basis of two scalable architectures for flux qubits taking into account crosstalk, incorporation of classical control circuitry, power dissipation, and fault-tolerant considerations such as permitting a universal set of logical gates, parallelism, measurement and initialization, and data mobility.

I. INTRODUCTION

The field of quantum computation is largely concerned with the manipulation of two state quantum systems called qubits. Unlike the bits in today's computers which can be either 0 or 1, qubits can be placed in arbitrary superpositions $\alpha|0\rangle + \beta|1\rangle$, and entangled with each other. For a complete review of the basic properties of qubits and quantum information, see [2]. The attraction of quantum computation lies in the existence of quantum algorithms that are in some cases exponentially faster than their best known classical equivalents. Most famous are Shor's factoring algorithm [3] and Grover's search algorithm [4]. There has also been extensive work on using a quantum computer to simulate quantum physics [5, 6, 7, 8, 9], an ongoing exploration of adiabatic algorithms [10, 11, 12], plus the discovery of quantum algorithms for differential equations [13], finding eigenvalues [14, 15], numerical integration [16] and various problems in group theory [17, 18, 19] and knot theory [20, 21].

Quantum systems suffer from decoherence, meaning their state rapidly becomes unknowable through unwanted interaction with the environment. Flux qubit decoherence times of up to a few microseconds have been demonstrated [22] versus single-qubit gate times of order 10 ns and likely initial two-qubit gate times of order a few tens of nanoseconds [1, 23]. To perform long quantum computations, quantum error correction will be required [24, 25, 26]. It has been shown that provided the totality of decoherence and control errors is below some nonzero threshold, and given an arbitrarily long time and an arbitrary large number of qubits, an arbitrarily long and large quantum computation can be performed [27]. Despite being well known in certain circles, the broader quantum computing community has not yet sufficiently come to terms with the fact that long-range interactions permit much higher levels of decoherence and control error to be tolerated. With unlimited range interactions

and extremely large numbers of qubits, the threshold error rate has been shown to be of order 10^{-2} [28]. With fewer qubits but still unlimited range interactions, the threshold is reduced to between 10^{-3} and 10^{-4} [29]. A 2D lattice of qubits interacting with their nearest neighbors only has been devised with approximate threshold 10^{-5} [30]. The full analysis of an infinite double line of qubits with nearest neighbor interactions has been performed yielding a lower bound to the threshold of 1.96×10^{-6} [31]. Work on an infinite single line of qubits with nearest neighbor interactions is in progress, and the threshold is expected to be of order 10^{-8} [32].

Despite the extremely low expected threshold of linear nearest neighbor (LNN) architectures, a great deal of theoretical work has been devoted to the design of such architectures using a variety of physical systems [33, 34, 35, 36, 37, 38, 39, 40, 41, 42, 43]. This is reasonable in the context of providing an experimental starting point, but we believe the time has come to expect at least a theoretical proposal for how long-range interactions or long-distance qubit transport might be performed. Without this, it is extremely difficult to argue the long-term viability of a given system. Furthermore, any proposed method of interaction or transport must be able to be performed in parallel on a number of pairs of qubits that grows linearly with the size of the computer to permit the simultaneous application of error correction to a constant fraction of the logical qubits in the computer. By contrast, a quantum computer based around a single, global, serial interaction or transport mechanism, such as a single resonator shared by all qubits in the computer, cannot simultaneously apply quantum error correction to multiple logical qubits. Such a quantum computer could at best apply quantum error correction to each logical qubit in turn. As the number of logical qubits increases and the amount of time between applications of error correction to a given logical qubit increases, more errors accumulate and the probability of successful error correction de-

creases. Beyond a certain amount of time between error correction applications, it is overwhelmingly likely that every physical qubit comprising a given logical qubit will have suffered an error, meaning no amount of quantum error correction will successfully recover the original logical state. Consequently, any quantum computer based around a single, global, serial interaction or transport mechanism is not scalable in the sense that it could never perform an arbitrarily large quantum computation.

The purpose of this paper is to present a long-range coupling mechanism for superconducting flux qubits that can be used to couple many pairs of qubits together in parallel in a manner suited to the construction of an arbitrarily large fault-tolerant quantum computer. In Section II we review the coupling mechanism of [1, 23] and extend it to allow long-range coupling. In Section III we firstly describe a simple, yet scalable, flux qubit architecture based on this interaction, but not taking full advantage of it, then a more complicated architecture with a better threshold error rate though much more difficult to build. Finally, Section IV concludes with a summary of results and a description of further work.

II. COUPLING FLUX QUBITS

Before discussing our coupling mechanism, a few words elaborating exactly why long-range interactions are advantageous are in order. Essentially, the problem lies in the need to perform transversal multiple logical qubit gates, as shown in Fig. 1a. If long-range interactions are available, two n physical qubit logical qubits can be transversely interacted in a single time step using n gates. If we now try to do the same thing on a linear nearest neighbor architecture using swap gates prior to the necessary gates to perform the transversal interaction, we immediately run into a serious problem. A single swap gate failure can lead to two errors in a single logical qubit as shown in Fig. 1b. Under normal circumstances, two or more errors in a single logical qubit are not correctable. A solution to this dilemma is shown in Fig. 1c where a second line of placeholder qubits has been added. Now swap gates never simultaneously touch two qubits that are both part of logical qubits. Note that the first three steps of Fig. 1c need to be repeated, time reversed, to return the qubits to their original configuration. We can now see that to interact two n qubit logical qubits transversely and fault-tolerantly using only nearest neighbor interactions, using the scheme described, we need $4n$ qubits, $2n^2 + n$ gates and $2n + 1$ time steps with $2n^2$ locations where data qubits are left idle. For all of this additional machinery to result in a circuit with the same reliability as the nonlocal case, every individual component must be significantly more reliable. This is the origin of the lower thresholds quoted in the introduction for ever more constrained architectures.

With the above motivation in mind, we proceed to the discussion of coupling superconducting flux qubits.

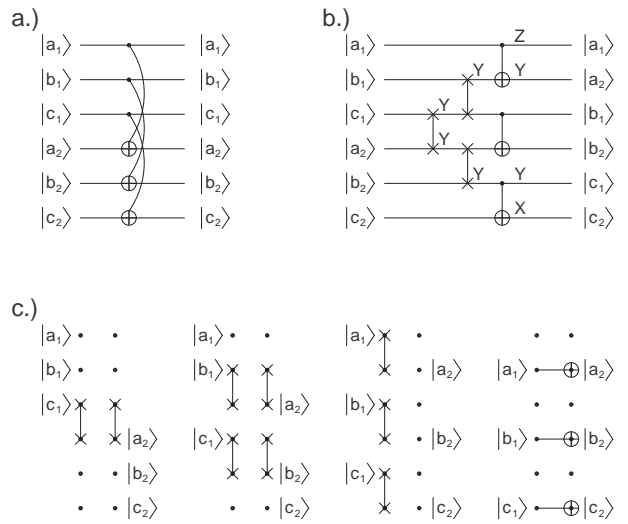


FIG. 1: a.) nonlocal transversal interaction, b.) naive linear nearest neighbor transversal interaction showing the propagation of errors resulting from the failure of a single swap gate leading to two errors in both logical qubits, c.) the first $n + 1$ time steps of a bilinear fault-tolerant transversal interaction. The remaining n steps are the time reverse of the first n steps.

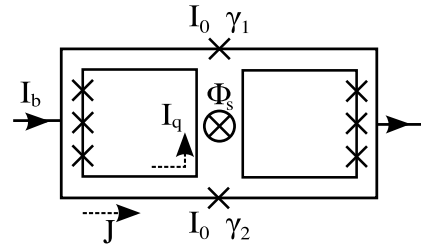


FIG. 2: Coupling scheme as proposed in [1], including circuit symbols and orientations.

Coherent oscillations of the state of a superconducting flux qubit were first demonstrated at Delft in 2003 [44]. A number of other institutions are also developing flux qubit technology, including Berkeley [23], NEC [45, 46], NTT [47] and IPHT [48]. A flux qubit is essentially a superconducting ring interrupted by typically three Josephson junctions with clockwise and anticlockwise persistent currents forming the basis of an effective two level quantum system. For an up-to-date review of superconducting qubit theory in general, including flux qubits, see [49].

The coupling scheme as proposed in [1] is shown, somewhat simplified, in Fig. 2. The strength of the direct inductive coupling between the qubits is given by $K_0 = 2M_{qg}I_q^2$, whereas that mediated by the SQUID takes the form

$$K_s = 2M_{qg}^2 I_q^2 \left(\frac{\partial J}{\partial \Phi_s} \right)_{I_b}. \quad (1)$$

In the slowly varying and high resistance limit of the junctions, we can write

$$I_b = I_0 \sin \gamma_1 + I_0 \sin \gamma_2, \quad (2)$$

$$2J = I_0 \sin \gamma_2 - I_0 \sin \gamma_1 \quad (3)$$

which can also be written as

$$I_b = 2I_0 \sin \bar{\gamma} \cos \Delta\gamma, \quad (4)$$

$$J = I_0 \sin \Delta\gamma \cos \bar{\gamma} \quad (5)$$

where $\Delta\gamma = \frac{\gamma_2 - \gamma_1}{2}$ and $\bar{\gamma} = \frac{\gamma_1 + \gamma_2}{2}$. These equations are constrained by

$$d\Delta\gamma = \frac{\pi}{\Phi_0} (d\Phi_s - LdJ) \quad (6)$$

where L is the inductance of the coupler and Φ_s is the applied flux. Taking the partial derivative of Eqs. (4), (5), and (6) with respect to Φ_s we obtain

$$\frac{\partial I_b}{\partial \Phi_s} = 0 = 2I_0 \frac{\partial}{\partial \Phi_s} (\cos \Delta\gamma \sin \bar{\gamma}), \quad (7)$$

$$\frac{\partial J}{\partial \Phi_s} = I_0 \left[-\frac{\partial \bar{\gamma}}{\partial \Phi_s} \sin \bar{\gamma} \sin \Delta\gamma + \frac{\partial \Delta\gamma}{\partial \Phi_s} \cos \bar{\gamma} \cos \Delta\gamma \right], \quad (8)$$

$$\frac{\partial \Delta\gamma}{\partial \Phi_s} = \frac{\pi}{\Phi_0} (1 - L \frac{\partial J}{\partial \Phi_s}). \quad (9)$$

Using these equations, we can derive the expression

$$\left(\frac{\partial J}{\partial \Phi_s} \right)_{I_b} = \frac{1}{2L_j} \frac{1 - \tan^2 \bar{\gamma} \tan^2 \Delta\gamma}{1 + \frac{L}{2L_j} (1 - \tan^2 \bar{\gamma} \tan^2 \Delta\gamma)} \quad (10)$$

where $L_j = \Phi_0 / (2\pi I_0 \cos \Delta\gamma \cos \bar{\gamma})$ is the Josephson inductance. This expression characterizes the tunable nature of the coupling scheme.

We propose modifying the coupler as shown in Fig. 3. All dimensions are typical of the Berkeley group [23]. This design results in decreased mutual inductance between the qubits, increased mutual inductance between the qubits and the coupler, increased self inductance of the coupler and significant capacitance structurally incorporated into the coupler. All of these effects will be investigated, and the resultant impact on the coupling strength.

Before discussing coupling strengths, we need to determine the various inductances of the new system. Fig. 4 shows the self inductance of the coupler versus coupler length D for coupler width $d = 1.5 \mu\text{m}$ generated using FastHenry. The inset shows the short length behavior. For all lengths of interest, the coupler self inductance is approximately given by $(356 + 0.863D/\mu\text{m}) \text{ pH}$. A small value of d is desirable to minimize L at a given length and, as we shall see, maximize the coupling strength. However, this also introduces a large capacitance, with consequences to be discussed at the end of this section.

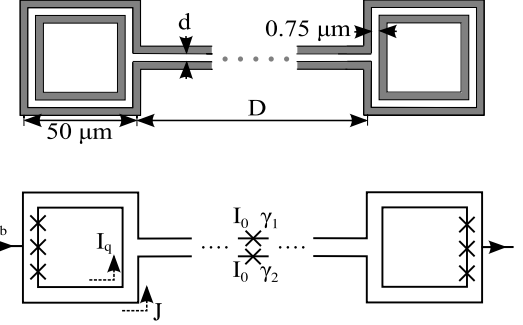


FIG. 3: Extending coupling scheme, including circuit symbols, orientations and dimensions. All wires are $0.75 \mu\text{m}$ wide and $0.2 \mu\text{m}$ thick

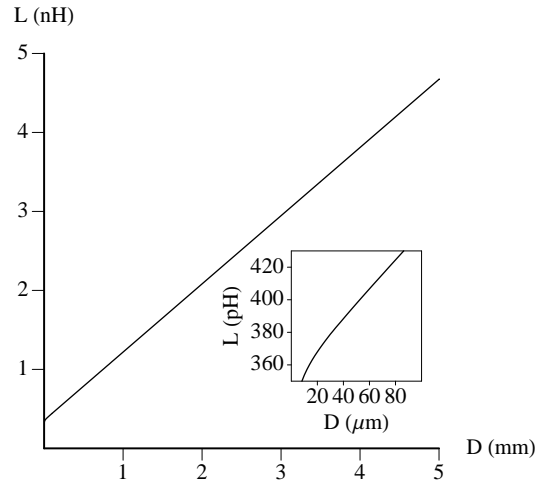


FIG. 4: The self-inductance of the coupler as a function of the length of the coupler.

The mutual inductance of each qubit with the coupler was found to be 75 pH .

We are now in a position to calculate the coupler mediated coupling strength K_s for zero bias current, done numerically for two different critical currents $I_0 = 0.48$ and $0.16 \mu\text{A}$ and shown in Fig. 5. Note the existence of optimum lengths, 700 and $3000 \mu\text{m}$ respectively, a consequence of the cosine terms in L_j . The coupling strength due to the mutual inductance of the qubits is shown in Fig. 6. Note that to neglect the direct coupling it is necessary for the coupler to be greater than approximately $650 \mu\text{m}$ long, corresponding to a coupling strength approximately 3 orders of magnitude less than that mediated by a short coupler. The consequences of this for architecture design are discussed in Section III.

The coupling strength can be reduced to zero by sufficiently increasing the bias current. It is desirable to ensure that the necessary increase is as small as possible, as the presence of a bias current, particularly one close to

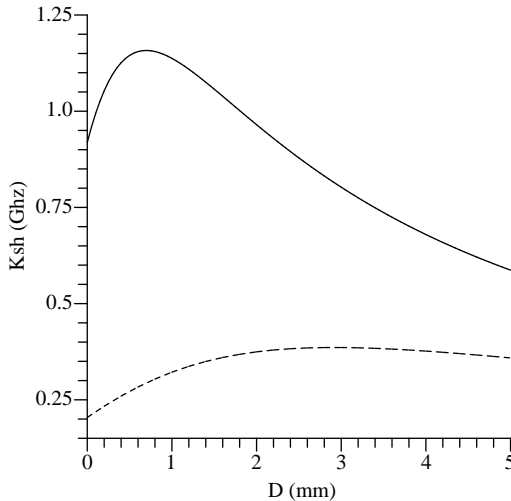


FIG. 5: The coupling strength at zero bias current without mutual qubit interaction versus the length of the coupler for $I_0 = 0.48 \mu\text{A}$ (solid) and $I_0 = 0.16 \mu\text{A}$ (dashed).

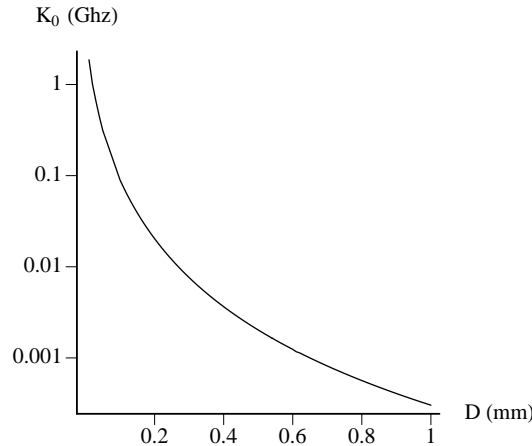


FIG. 6: The strength of the direct qubit-qubit interaction due to mutual inductive coupling as a function of the length of the coupler, and thus qubit separation.

the critical current, is a significant source of decoherence [1, 45, 50]. Fig. 7 shows the coupling strength versus bias current for a selection of four coupler lengths. This figure uses the critical current $I_0 = 0.48 \mu\text{A}$ from [1]. Clearly, particularly for long lengths, the bias current required to achieve zero coupling strength is too close to the critical current. This problem can be circumvented by reducing the critical current of the junctions to $I_0 = 0.16 \mu\text{A}$ resulting in Fig. 8. Reducing the critical current reduces the zero bias coupling strength lowering the ratio I_b/I_c required to achieve zero coupling strength.

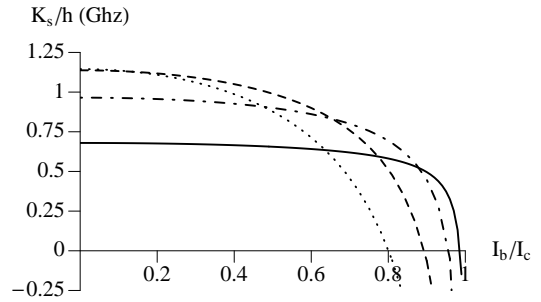


FIG. 7: The coupling strength as a function of the bias current, using Josephson Junction critical currents of $I_0 = 0.48 \mu\text{A}$. $D = 500 \mu\text{m}$ (dotted), $D = 1000 \mu\text{m}$ (dashed), $D = 2000 \mu\text{m}$ (dash-dotted), and $D = 4000 \mu\text{m}$ (solid).

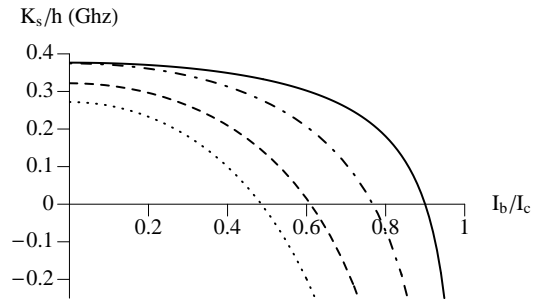


FIG. 8: The coupling strength as a function of the bias current, using Josephson Junction critical currents of $I_0 = 0.16 \mu\text{A}$. $D = 500 \mu\text{m}$ (dotted), $D = 1000 \mu\text{m}$ (dashed), $D = 2000 \mu\text{m}$ (dash-dotted), and $D = 4000 \mu\text{m}$ (solid).

In principle, Fig. 8 is promising, both in terms of coupling strength and coupling length. However, the effect of the capacitance of the coupler must be determined. As a starting point, consider a single flux qubit initially prepared in a clockwise current state. Left alone, this qubit will oscillate between clockwise and anticlockwise current states at its tunneling frequency, which is typically of order a few GHz in current devices. As seen by the coupler, by virtue of their mutual inductance, such a qubit plays the role of an alternating current source. Considering the coupler in isolation now, we wish to check that an alternating current source at one end of the coupler with amplitude A generates an alternating current of amplitude as close to A as possible at the other end. Using a lumped circuit model and discretizing the capacitive section of the coupler, deviation from perfect transmission of order 1% was found. This is low enough to give us confidence that the fundamental concept of the extended coupler is sound, but high enough that achieving high fidelity gates will require a closer examination of the physics of the system [51]. This will be discussed in detail in a separate publication.

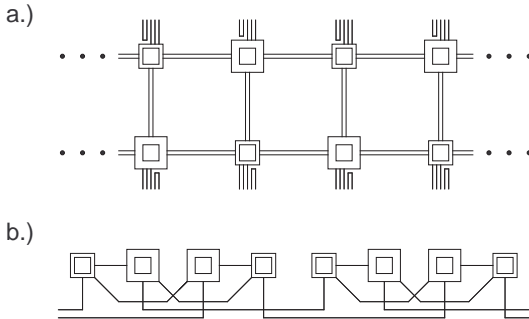


FIG. 9: Simple scalable flux qubit architecture. a) Bilinear array b) Topologically identical array used as the basis of Fig. 12.

III. ARCHITECTURES

In quantum computing literature, the word “scalable” is, regrettably, frequently used rather loosely, and sometimes inaccurately. Ideally, as a minimum, it should only be claimed that an architecture is scalable if in principle an arbitrarily large number of qubits can be implemented, the number of quantum gates and measurements that can be executed simultaneously grows linearly with the number of qubits, and the physics of any one quantum gate or measurement does not depend on the total number of qubits. A simple example of such an architecture making use of the coupler described in this paper is shown, not drawn to scale, in Fig. 9a. This architecture requires three couplers around each qubit, well within current layering technology. Note that one qubit of each pair is more weakly coupled following [23]. This enables readout of both qubits simultaneously using one coupler via the resonant readout scheme of [52]. Given the large potential length of each coupler, crosstalk can be neglected, and with just five wires per qubit leading to external generators and meters, given a sufficiently long fridge, possibly as shown in Fig. 10, heating issues can also be neglected. Two lines of qubits have been incorporated to permit simpler error correction resulting in a threshold two-qubit gate error rate for arbitrarily large fault-tolerant quantum computation of 1.96×10^{-6} as described in [31]. Note that to use this architecture in practice this implies the need for two-qubit gates operating with an error rate of 10^{-7} or less, far below what is achievable in most solid-state systems given the current ratios of decoherence times to gate times.

Of course, the architecture of Fig. 9a does not take full advantage of the potential length of the coupler. As discussed earlier, to ensure relatively low crosstalk, from Fig. 4, qubits need to be spaced approximately $650 \mu\text{m}$ apart. This still gives us enough space to firstly stretch the architecture of Fig. 9a into a single line as shown in Fig. 9b, then duplicate this line 7 times to permit an additional layer of the 7-qubit Steane code to be used. Referring to Fig. 12, these duplicated qubits correspond

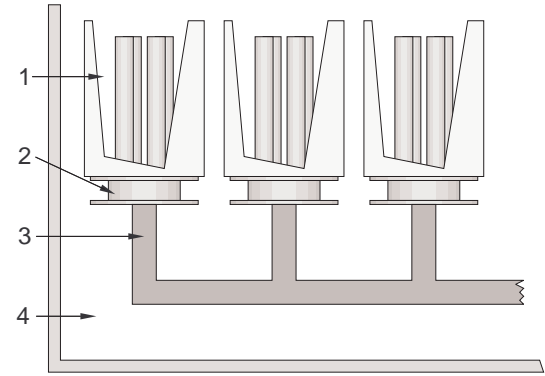


FIG. 10: A dilution fridge making use of multiple mixing chambers. 1: 1 K liquid helium, 2: Mixing chamber, 3: mK copper support structure, 4: Vacuum.

to the bottom seven qubits in each group of 21. The middle row of qubits in each group of 21 correspond to ancilla qubits used during error correction according to the scheme described in [26], with slight modifications to reduce the range of the necessary interactions as shown in Fig. 11. The top row of qubits in each group of 21 correspond to ancilla qubits only used during the implementation of the fault-tolerant T gate, or $\pi/8$ gate, as it is also known, which is required to ensure the computer can perform a universal set of fault-tolerant gates. A complete description of the circuitry of this gate can be found in [31]. Note that, even with all the additional control lines, the architecture requires just one wire per $50 \mu\text{m}$ per side.

The network of qubits and couplers shown in Fig. 12 enables the most efficient known nonlocal error correction scheme and fault-tolerant gates to be implemented at the lowest level. All higher levels make use of the circuitry devised for the bilinear architecture. When the threshold two-qubit error rate of this more complicated architecture was calculated, the disappointingly low result of 6.25×10^{-6} was obtained — just over a factor of three better than the bilinear array. In short, the dominant nearest neighbor behavior of the large-scale architecture is not overcome by a single layer of nonlocal error correction and gates.

IV. CONCLUSION

We have described in detail a nonlocal method of coupling pairs of flux qubits and shown that it is suited to the construction of complex, scalable quantum computer architectures as shown in Fig. 12. By virtue of the fact that flux qubits do not require large quantities of classical control circuitry on chip, there are no obvious lithographic or heat dissipation barriers to the construction of such an architecture. The primary concern, as with all superconducting quantum technology, is decoherence. In

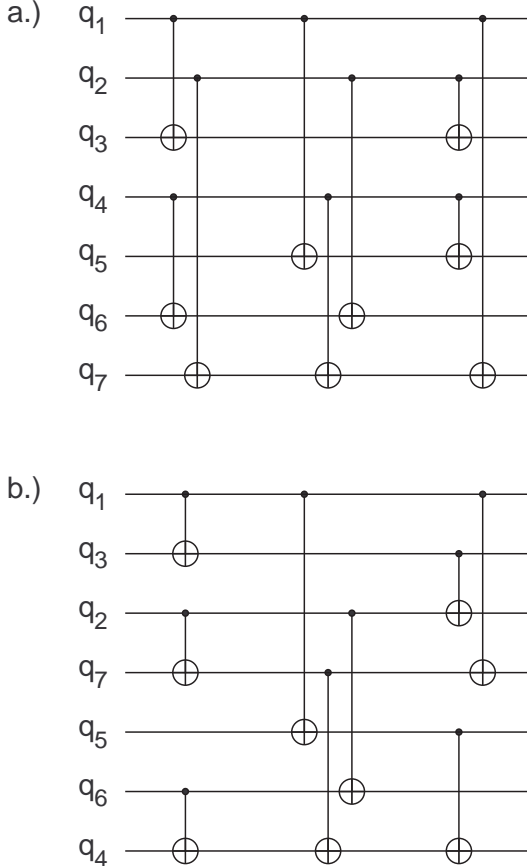


FIG. 11: To reduce the need for long range interactions, the circuit a.) taken from [26] was modified as shown in b.) by swapping two pairs of qubits.

the near future we wish to look at other superconducting qubits and coupling schemes with the aim of removing all known sources of decoherence from the design. For example, in [45] a method of coupling flux qubits tunably is described that does not resort to a nonzero SQUID bias current. Furthermore, the need for large qubit separations to minimize crosstalk could in principle be alleviated by enclosing each qubit in a micrometer scale Faraday cage. Devising a more practical method of achieving higher qubit densities would greatly increase the utility of the proposed coupling scheme. Finally, with or without higher qubit densities, additional architecture design work is required to try to raise the threshold further, possibly by attempting to incorporate two layers of nonlocal error correction into the design.

V. ACKNOWLEDGEMENTS

AGF and FKW would like to thank B. Plourde and S. Oh for helpful discussions. This work was supported by an NSERC Discovery Grant and the European Union through EuroSQIP.

[1] B. L. T. Plourde, J. Zhang, K. B. Whaley, F. K. Wilhelm, T. L. Robertson, T. Hime, S. Linzen, P. A. Reichardt, C.-E. Wu, and J. Clarke, *Phys. Rev. B* **70**, 140501 (2004), quant-ph/0406049.

[2] M. A. Nielson and I. L. Chuang, *Quantum Computation and Quantum Information* (Cambridge University Press, Cambridge, 2000).

[3] P. W. Shor, in *Proc. 35th Annual Symposium on Foundations of Computer Science* (1994), pp. 124–134.

[4] L. K. Grover, in *Proc. Twenty-Eighth Annual ACM Symposium on the Theory of Computing* (1996), pp. 212–219, quant-ph/9605043.

[5] R. P. Feynman, *Int. J. Theor. Phys.* **21**, 467 (1982).

[6] S. Lloyd, *Science* **273**, 1073 (1996).

[7] B. M. Boghosian and W. Taylor, *Physica D* **120**, 30 (1998), quant-ph/9701019.

[8] A. T. Sornborger and E. D. Stewart, *Phys. Rev. A* **60**, 1956 (1999), quant-ph/9903055.

[9] T. Byrnes and Y. Yamamoto, *Phys. Rev. A* **73**, 022328 (2006), quant-ph/0510027.

[10] E. Farhi, J. Goldstone, S. Gutmann, J. Lapan, A. Lundgren, and D. Preda, *Science* **292**, 472 (2001), quant-ph/0104129.

[11] A. M. Childs, E. Farhi, J. Goldstone, and S. Gutmann, *Quant. Info. Comp.* **2**, 181 (2002), quant-ph/0012104.

[12] M. C. Banuls, R. Orus, J. I. Latorre, A. Perez, and P. Ruiz-Femenia, *Phys. Rev. A* **73**, 022344 (2006), quant-ph/0503174.

[13] T. Szkopek, V. Roychowdhury, and E. Yablonovitch, quant-ph/0408137 (2004).

[14] D. S. Abrams and S. Lloyd, *Phys. Rev. Lett.* **83**, 5162 (1999), quant-ph/9807070.

[15] P. Jaksch and A. Papageorgiou, *Phys. Rev. Lett.* **91**, 257902 (2003), quant-ph/0308016.

[16] D. S. Abrams and C. P. Williams, quant-ph/9908083 (1999).

[17] A. Y. Kitaev, Tech. Rep. TR96-003, Electronic Colloquium on Computational Complexity (1996), quant-ph/9511026.

[18] M. Mosca and A. Ekert, *Lecture Notes in Computer Science* **1509**, 174 (1999), quant-ph/9903071.

[19] S. A. Fenner and Y. Zhang, in *Proc. 9th IC-EATCS Italian Conference on Theoretical Computer Science* (2005), pp. 215–227, quant-ph/0408150.

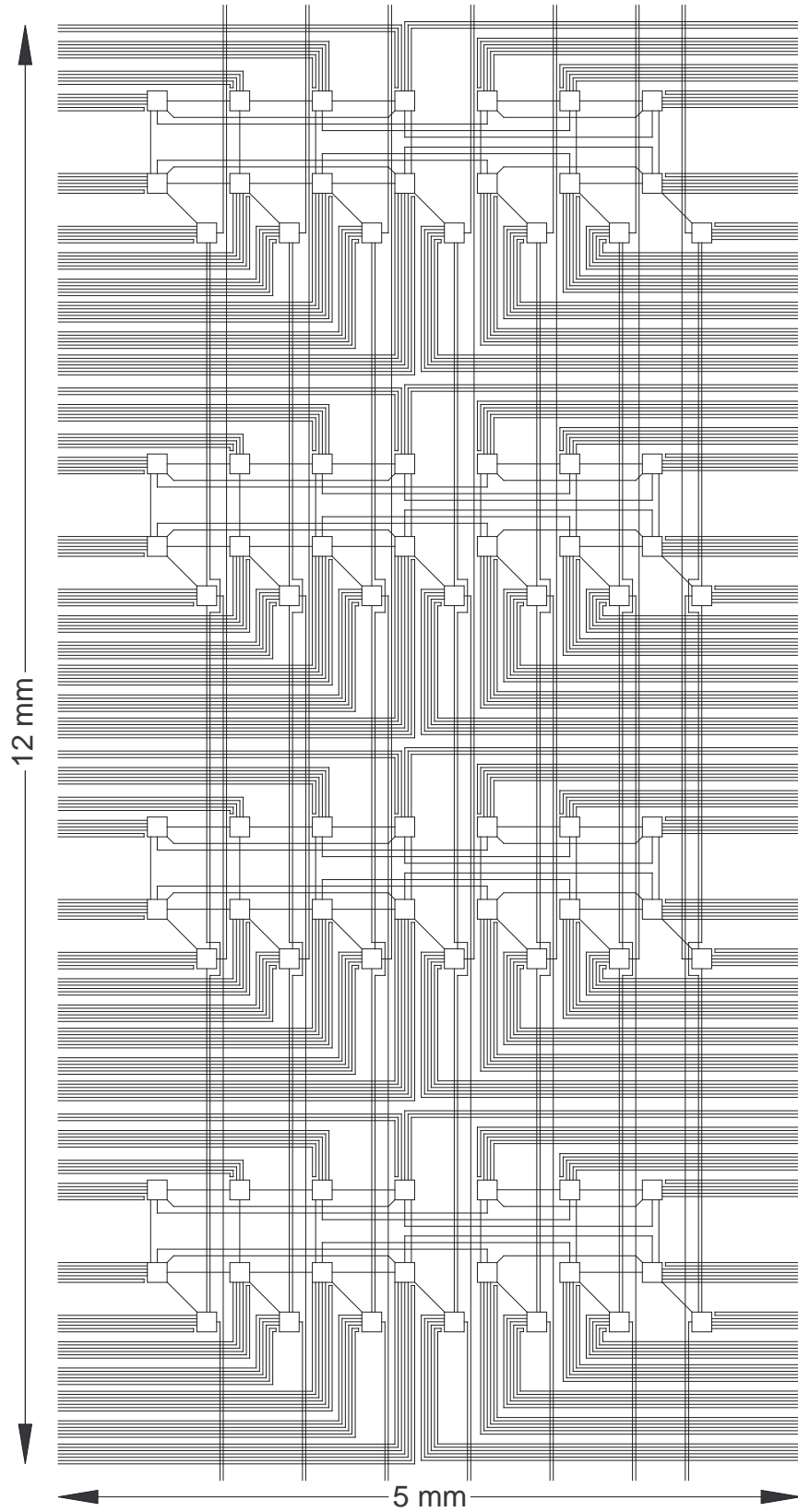


FIG. 12: A complete architecture for a flux qubit quantum computer. Squares represent flux qubits, lines connecting squares represent SQUID couplers, lines running away from each square represent squid bias current lines and flux bias lines. The size of the flux qubits has been exaggerated for clarity.

[20] V. Subramaniam and P. Ramadevi, quant-ph/0210095 (2002).

[21] P. Wocjan and J. Yard, quant-ph/0603069 (2006).

[22] P. Bertet, I. Chiorescu, G. Burkard, K. Semba, C. J. P. M. Harmans, D. P. DiVincenzo, and J. E. Mooij, Phys. Rev. Lett. **95**, 257002 (2005), cond-mat/0512428.

[23] T. Hime, P. A. Reichardt, B. L. T. Plourde, T. L. Robertson, C.-E. Wu, A. V. Ustinov, and J. Clarke, Science **314**, 1427 (2006).

[24] A. R. Calderbank and P. W. Shor, Phys. Rev. A **54**, 1098 (1995), quant-ph/9512032.

[25] A. M. Steane, Proc. R. Soc. Lond. A **425**, 2551 (1996), quant-ph/9601029.

[26] D. P. DiVincenzo and P. Aliferis, Phys. Rev. Lett. **98**, 020501 (2007), quant-ph/0607047.

[27] E. Knill, R. Laflamme, and W. H. Zurek, Tech. Rep. LAUR-96-2199, Los Alamos National Laboratory (1996), quant-ph/9610011.

[28] E. Knill, quant-ph/0410199 (2004).

[29] A. M. Steane, Phys. Rev. A **68**, 042322 (2003), quant-ph/0207119.

[30] K. M. Svore, D. DiVincenzo, and B. Terhal, Quant. Info. Comp. **7**, 297 (2007), quant-ph/0604090.

[31] A. M. Stephens, A. G. Fowler, and L. C. L. Hollenberg, quant-ph/0702201 (2007).

[32] A. M. Stephens, A. G. Fowler, and L. C. L. Hollenberg (2007), in preparation.

[33] N.-J. Wu, M. Kamada, A. Natori, and H. Yasunaga, Jpn. J. Appl. Phys. **39**, 4642 (2000), quant-ph/9912036.

[34] R. Vrijen, E. Yablonovitch, K. Wang, H. W. Jiang, A. Balandin, V. Roychowdhury, T. Mor, and D. DiVincenzo, Phys. Rev. A **62**, 012306 (2000), quant-ph/9905096.

[35] B. Golding and M. I. Dykman, cond-mat/0309147 (2003).

[36] E. Novais and A. H. C. Neto, Phys. Rev. A **69**, 062312 (2004), cond-mat/0308475.

[37] L. C. L. Hollenberg, A. S. Dzurak, C. Wellard, A. R. Hamilton, D. J. Reilly, G. J. Milburn, and R. G. Clark, Phys. Rev. B **69**, 113301 (2004), cond-mat/0306235.

[38] L. Tian and P. Zoller, Phys. Rev. A **68**, 042321 (2003), quant-ph/0306085.

[39] M. Friesen, P. Rugheimer, D. E. Savage, M. G. Lagally, D. W. van der Weide, R. Joynt, and M. A. Eriksson, Phys. Rev. B **67**, 121301 (2003), cond-mat/0208021.

[40] L. M. K. Vandersypen, R. Hanson, L. H. W. van Beeren, J. M. Elzerman, J. S. Greidanus, S. D. Franceschi, and L. P. Kouwenhoven, in *Quantum Computing and Quantum Bits in Mesoscopic Systems*, edited by A. J. Leggett, B. Ruggiero, and P. Silvestrini (Kluwer Academic/Plenum Publishers, New York, 2003), quant-ph/0207059.

[41] P. Solinas, P. Zanardi, N. Zanghi, and F. Rossi, Phys. Rev. B **67**, 121307 (2003), quant-ph/0207019.

[42] V. V'yurkov and L. Y. Gorelik, Quant. Comput. and Comput. **1**, 77 (2000), quant-ph/0009099.

[43] E. O. Kamenetskii and O. Voskoboinikov, cond-mat/0310558 (2003).

[44] I. Chiorescu, Y. Nakamura, C. J. P. M. Harmans, and J. E. Mooij, Science **299**, 1869 (2003), cond-mat/0305461.

[45] A. O. Niskanen, Y. Nakamura, and J.-S. Tsai, Phys. Rev. B **73**, 094506 (2006), cond-mat/0512238.

[46] A. O. Niskanen, K. Harrabi, F. Yoshihara, Y. Nakamura, and J.-S. Tsai, Phys. Rev. B **74**, 220503(R) (2006), cond-mat/0609627.

[47] K. Kakuyanagi, T. Meno, S. Saito, H. Nakano, K. Semba, H. Takayanagi, F. Deppe, and A. Shnirman, Phys. Rev. Lett. **98**, 047004 (2007), cond-mat/0609564.

[48] M. Grajcar, A. Izmalkov, , and E. Illichev, Phys. Rev. B **71** (2005), cond-mat/0407405.

[49] M. R. Geller, E. J. Pritchett, A. T. Sornborger, and F. K. Wilhelm, quant-ph/0603224 (2006).

[50] C. H. van der Wal, F. K. Wilhelm, C. J. P. M. Harmans, and J. E. Mooij, Eur. Phys. J. B **31**, 111 (2003), cond-mat/0211664.

[51] C. Hutter, A. Shnirman, Y. Makhlin, and G. Schn, Euphys. Lett. **74**, 1088 (2006), cond-mat/0602086.

[52] I. Serban, E. Solano, and F. K. Wilhelm (2007), in preparation.